ELSEVIER

Journal of Molecular Graphics and Modelling 20 (2001) 245–256

Journal of Molecular Graphics and Modelling

www.elsevier.com/locate/JMGM

Conformational analysis of thiopeptides: free energy calculations on the effects of thio-substitutions on the conformational distributions of alanine dipeptides

Tran Trung Tran*, Antony W. Burgess, Herbert Treutlein, Jun Zeng

Ludwig Institute for Cancer Research, Cooperative Research Center for Cellular and Growth Factors, Royal Melbourne Hospital, P.O. Box 2008, Parkville, Vic. 3050, Australia

Received 1 March 2001; received in revised form 11 June 2001; accepted 18 June 2001

Abstract

When the oxygen atom in a peptide bond is replaced by a sulfur atom, the restriction in the available conformational space and the ability of thioamides to confer resistance to enzymatic degradation renders thioamides as potentially useful building blocks for drug design and protein engineering. The solvation free energy differences between conformers of the same dipeptide can be high. Yet, previous conformational studies, basing on the (ϕ, ψ) conformational energy maps of thio-substituted dipeptides, neglected both explicit water interactions and free energy considerations. In this paper, the (ϕ, ψ) conformational free energy maps are obtained by single umbrella sampling in an explicit water environment for both alanine dipeptide and the corresponding thioamide derivatives.

The ϕ and ψ angles for the minima in the relative energy maps calculated with dielectric of 80 are similar to the corresponding ϕ and ψ angles in the relative free energy maps for both Ac-Ala-NHMe (Ac: acetyl; Ala: alanine) and Act-Alat-NHMe (Act: thio-acetyl; Alat: thio-alanine). However, some large differences between the relative energy and relative free energy of major minima indicate that the consideration of free energy is important in determination of the relative occupancy of particular minima.

Free energy maps for both Ac-Ala-NHMe and Act-Alat-NHMe show that thio-substitution favors conformations where $\phi < 0$ because of the deeper β and α_R minima. The changes in the position and relative stability of minima were explained in terms of the destabilization of the regions near $\phi = -120$, 0 and 120, $\psi = 60$, -60, 180, which correspond to the increased steric hindrance due to the bulkier sulfur atom.

Keywords: Thioamides; Free energy; Ramanchandran plot; Non-natural amino acids; Uncoded amino acids; Conformationally restricted amino acids; Dipeptide and umbrella sampling

1. Introduction

Non-natural amino acids have been used in protein engineering and drug design for many purposes: to confer resistance to enzymatic degradation [1–3], to probe the functions of protein structure [4–6], in the process of de novo design [7–12], to design structures with novel folds or secondary structure [13,14], to create new combinatorial chemistry libraries [15] and to allow more predictable peptide conformers to be constructed with potentially increased binding affinity to proteins [7,16–19]. To extend the repertoire of non-natural amino acids that can be exploited, the conformational implications of replacing the oxygen atom in a peptide unit with a bulkier sulfur atom, forming thiopeptides, have been explored [2,20–27].

The (ϕ, ψ) conformational energy maps have been constructed for thiopeptides using a hard-sphere model and extended Hückel theory [21], a rigid geometry force field ECEPP/2 [2], the MM2 force field [24] and the extended CFF91 force field as described in previous papers of this series [25–27]. The results of those calculations show that thio-substitution does restrict the conformations available to thiopeptides compared to peptides. Since solvation free energy differences between conformers of the same dipeptide can be as high as 10 kcal/mol for the enthalpic contribution and 8 kcal/mol for the entropic contribution [28–33] and previous conformational studies of thio-substituted dipeptides neglected both explicit water interactions and free energy considerations, this paper aims to calculate the (ϕ, ψ) maps using an explicit water model and furthermore, the calculations are extended to calculate the free energy of the

* Corresponding author. Present address: Institute of Molecular Bioscience, University of Queensland, St. Lucia, Brisbane, Qld 4072, Australia. Tel.: +61-7-33651292; fax: +61-7-33651900.
E-mail address: t.tran@mailbox.uq.edu.au (T.T. Tran).

1093-3263/01/$ – see front matter
PII: S1093-3263(01)00118-8

system, so that the effects of entropy to the conformational distribution can be considered.

Anderson and Hermans [34] calculated the free energy differences between four observed minima, β, α_L, C_7^{axial} and α_R region of Ac-Ala-NHMe (Ac: acetyl; Ala: alanine) using the molecular dynamics (MD) and thermodynamic integration (TI) [35] along a chosen dihedral angle coordinate. Tobias and Brooks [32] used MD simulations with holonomic backbone dihedral angle constraints and thermodynamic perturbation (TP) [35,36] theory to calculate free energy profiles along the paths which connected four important minima for Ac-Ala-NHMe in the gas phase and in water. In contrast, umbrella sampling [37–39] is used in this study to calculate the free energy of the alanine and thio-substituted alanine dipeptide conformations.

The TI by Anderson and Hermans [34] and TP by Tobias and Brooks [32] rely on the calculations of potential of mean force between the four minima. In principle, the free energy difference between two states is independent of the path chosen to connect them since free energy is a thermodynamic state function [40]. However, in practice, with limited equilibration and sampling of some MD simulations, the choice of reaction pathway can influence the accuracy of the free energy estimation [38]. To avoid this potential problem, we aimed to remove the choice of reaction pathway by finding a single biasing function which would allow sampling of most of the (ϕ, ψ) conformational free energy surface in a single window. This sampling technique offers another advantage in that most of the (ϕ, ψ) free energy surface, minima and transition states are simulated.

To analyze the free energy map in terms of microscopic interactions, we decomposed the free energy differences into their entropic and energy components which are further decomposed into peptide–peptide (uu) and peptide–solvent (uv) components.

2. Methods

2.1. Choice of water model

Many models have been proposed to simulate liquid water in molecular mechanics calculations [41]. Five models with rigid water geometry are ST2 [42], Bernal–Fowler (BF) [43], SPC [44], TIP3P [41] and TIP4P [41]. To remain consistent with the previously derived thioamide CFF91 parameters [25–27], CFF91 water was used in our calculations. The CFF91 parameters have been derived and tested by other authors for protein and nucleic acid simulations [45–52].

2.2. Umbrella sampling

One of the major problems with free energy calculations is associated with insufficient sampling of conformations, especially high-energy conformations or systems with high-energy barriers between favorable conformations. In umbrella sampling, the Hamiltonian of the system is modified by the addition of a weighting function, $W(\xi)$, so that the sampling is biased towards the desired value of the chosen coordinate ξ. The Boltzmann average can be extracted from the biased non-Boltzmann distribution using a method introduced by Torrie and Valleau [37] and Northrup et al. [53].

$$w(\xi) = -k_B T \ln P_W(\xi) - W(\xi) + C$$

where $P_W(\xi)$ is the biased or weighted probability and $w(\xi)$ is the free energy surface along a chosen coordinate ξ. The third term, C, can be calculated indirectly by overlapping the free energy of different windows to satisfy the continuous nature of the free energy in the PMF. However, since single window umbrella sampling is used here and we are interested in obtaining only the relative free energy, the third term can be omitted.

2.3. Weighting function to bias the sampling

To sample the major regions of the (ϕ, ψ) conformational surface of the alanine dipeptide in a single window, a weighting function was needed which would allow crossing over major high-energy barriers in the (ϕ, ψ) surface under MD simulations at 300 K. The two high-energy barriers between the minima on the (ϕ, ψ) conformational energy map for Ac-Ala-NHMe [26] are the bridging regions at $(0°, 90°)$ or at $(0°, -90°)$ (defined here as *bridge* 1 and *bridge* 2, respectively). A plot of the energy barrier for the bridge 2 region is drawn (see http://www.ludwig.edu.au/archive/tran) and an energy barrier of 5.5 kcal/mol is seen. According to the equipartition theorem [40], the average energy of a particle is $(3/2)kT = 0.89$ kcal/mol at 300 K. Since the bridge 2 energy barrier is much larger than $(3/2)kT$, under MD at 300 K, the chance of crossing this barrier spontaneously is very low. The other barriers, between α_L and β region or between α_R and C_7^{axial} region are in the order of 1–2 kcal/mol, they would be expected to be traversed spontaneously. Therefore, a function which will lower the barrier at the $\phi = 0$ region should be sufficient to allow crossing over of all the major barriers between minima and, therefore, enable sampling of most low-energy regions of the (ϕ, ψ) conformational surface. A weighting function with this desired property was arbitrarily chosen from potential functions. The weighting function chosen for umbrella sampling of Ac-Ala-NHMe is (in rad)

$$W(\phi) = F_c[0.5\cos(3\phi) + 2\cos(2\phi) + 3\cos(\phi - 0.4)]$$

where F_c is the force constant equal to -0.7 kcal/mol. The graph for $W(\phi)$ is plotted in Fig. 1. Similar examinations were undertaken for the major energy barriers in the (ϕ, ψ) conformational energy maps for Act-Alat-NHMe (Act: thio-acetyl; Alat: thio-alanine). A similar weighting function with larger force constant of -0.9 was found to be appropriate for the umbrella sampling of Act-Alat-NHMe as the energy barrier for Act-Alat-NHMe is slightly higher than that for Ac-Ala-NHMe.

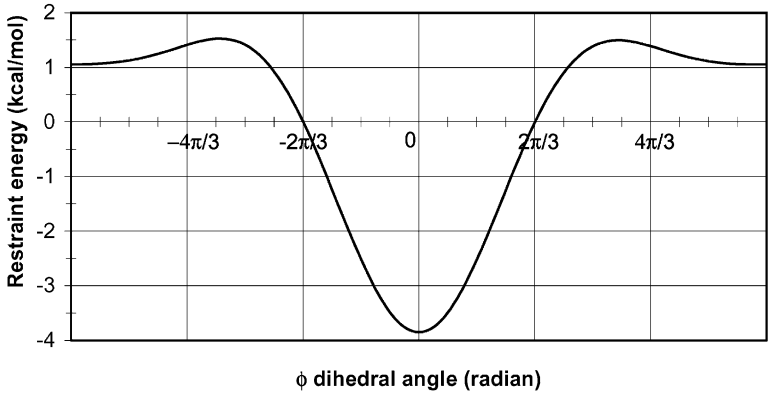

Fig. 1. Weighting function $W(\phi) = -0.7[0.5\cos(3\phi)+2\cos(2\phi)+3\cos(\phi-0.4)]$ used for the umbrella sampling of the (ϕ, ψ) conformational distributions for Ac-Ala-NHMe.

2.4. MD simulations

Each of Ac-Ala-NHMe and Act-Alat-NHMe dipeptide was placed in a cubic box of dimension 22 Å. Each of the boxes was filled with 339 water molecules to obtain an approximate density of 1 g/cm^3. MD simulations were run using the CDiscover program [54]. The CFF91 force field and the thioamide parameters derived from previous paper [25–27] of this series were used. Simulations were performed with periodic boundary condition and a cut-off distance of 11 Å. A group-based cut-off was used with a spline width of 1.0 Å and buffer width of 0.5 Å. MD simulations were performed at 300 K with constant volume and temperature. The temperature was kept constant by velocity scaling and the integration method was velocity verlet [54]. A time step of 1 fs was employed for the calculations with a sampling rate of the ϕ, ψ angle at every 1 fs and energy at every 100 fs. To obtain an indication of the extent and adequacy of the samplings, two runs were performed for each molecule starting from two different conformations. The 'duplicated' dynamic runs were monitored periodically for convergence and were stopped at approximately 4.3 ns.

2.5. Decomposition of the free energy

The energetic contribution to the free energy can be decomposed into the peptide–peptide, peptide–water and water–water components. Where possible, this decomposition can be calculated from the trajectory files obtained from the free energy calculation. However, due to limited computing resource, the thermodynamic decomposition of the free energies was performed using trajectory files obtained from short MD with light restraints to the β, α_R, α_L and extended minima. The restraint force constants used were 0.065 kcal/(torsional angle, °)^2 for the C_5 conformations and 0.016 kcal/(torsional angle, °)^2 for the other three conformations. Each MD simulations (similar conditions as the free energy calculation) were run for 70 ps and the coordinates were saved at every 15 fs. The peptide–peptide, peptide–water and water–water components of the energy were obtained from the trajectories using the CDiscover [54] program. Ensemble average and standard deviations of these components were computed for each minimum.

3. Results

3.1. MD simulations and sufficiency of sampling

Two tests were performed to examine the adequacy of sampling for the free energy calculations: (1) the ϕ and ψ dihedral angles were plotted against time to ensure a reasonable number of crossovers between the major minima on the (ϕ, ψ) map and (2) duplicated umbrella samplings from different starting conformations were performed for Ac-Ala-NHMe and Act-Alat-NHMe. If the resulting free energy maps obtained from the 'duplicated' runs were similar, this was taken as an indication that the sampling was sufficient.

The distributions of the ϕ, ψ dihedral angles of Ac-Ala-NHMe during MD simulations are plotted against each other and against time (Fig. 2). The figure shows that the ϕ dihedral angles have three high probability areas at 60 ± 25, -60 ± 25 and -160 ± 25. The ψ dihedral angles also have three high probability areas at -40 ± 25, 60 ± 25 and 155 ± 25. The time plots show that the ϕ, ψ angles moved in and out of each high probability area to other high probability areas at least 13 times during the 4.3 ns molecular dynamic simulation. Similar plots for Act-Alat-NHMe also shown that the each high probability area were visited for at least 10 times during the 4.3 ns molecular dynamic simulation.

The (ϕ, ψ) conformational free energy maps for Ac-Ala-NHMe and Act-Alat-NHMe were calculated from the (ϕ, ψ) distribution according to Section 2 and are plotted in Fig. 3. A bin in the (ϕ, ψ) energy or free energy map is a minimum when the energy is more than 0.6 kcal/mol (kT at 300 K) lower than the energy of the surrounding bins. If the barrier between two minima is <0.6 kcal/mol, it is considered as one minimum. Table 1 shows the ϕ, ψ dihedral angles and the relative free energy of the local minima and other interesting conformations from runs 01 and 02 and the

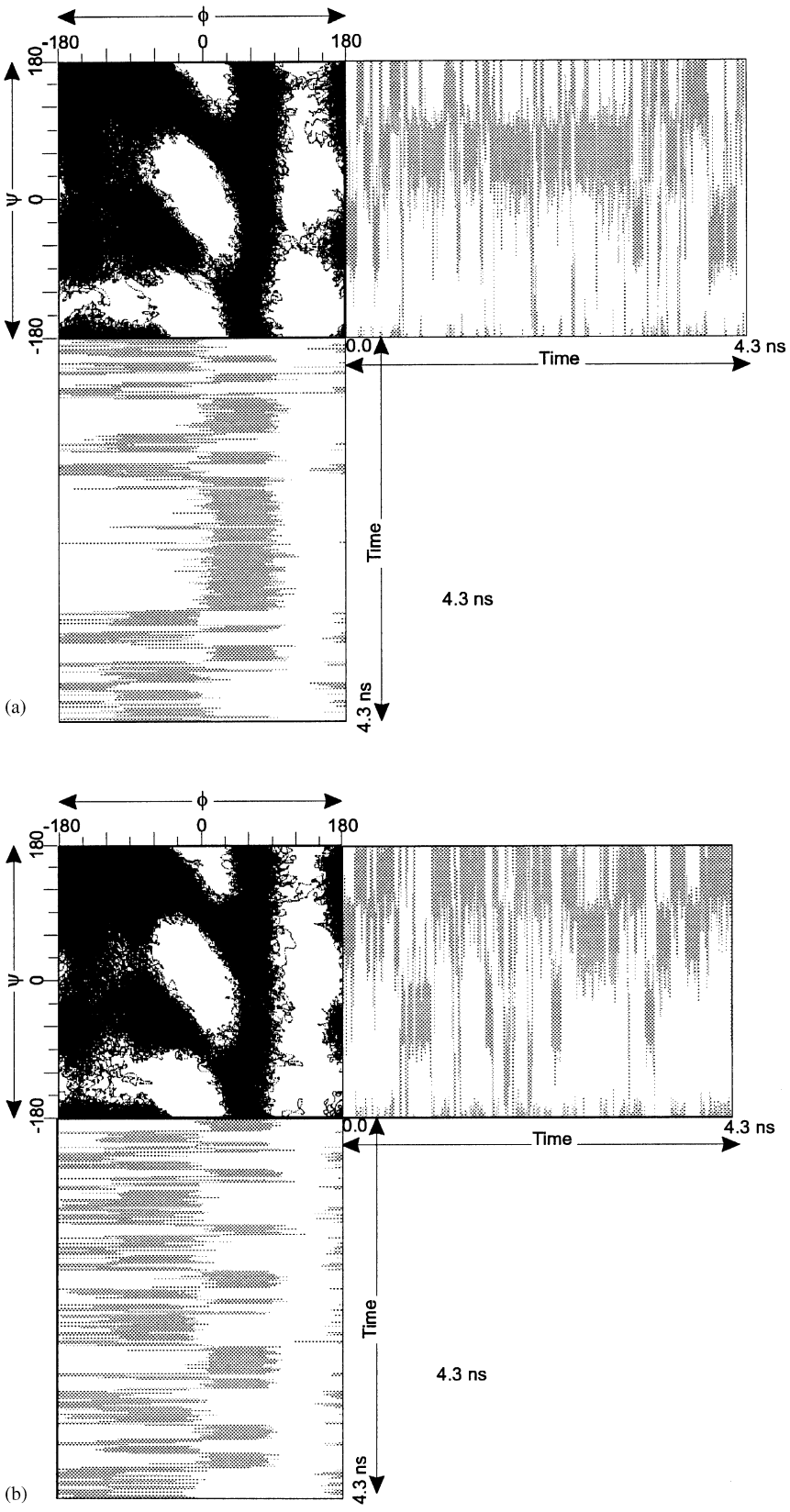

Fig. 2. Variations in the ϕ and ψ dihedral angles of Ac-Ala-NHMe during the molecular dynamics simulations: (a) run 01 and (b) run 02. The ϕ vs. ψ plot are in black and the ϕ or ψ vs. time plots are in grey.

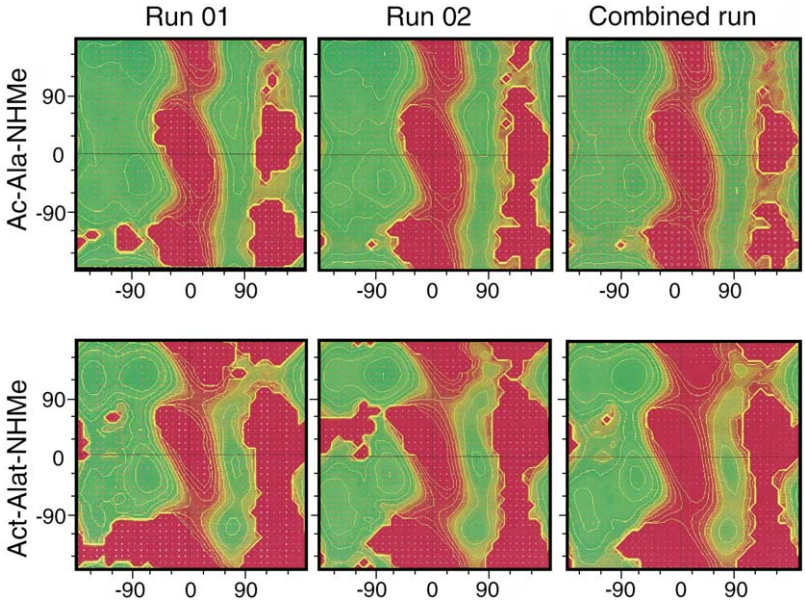

Fig. 3. Plots of free energy vs. ϕ and ψ dihedral angle for runs 01 and 02 and the combined results for Ac-Ala-NHMe and Act-Alat-NHMe dipeptides. Adjacent iso-free energy contour lines differ by 1 kcal/mol. The maps are colored green in low-energy regions and red in high-energy regions.

combined runs for Ac-Ala-NHMe and Act-Alat-NHMe. The ϕ and ψ angles for the minima of runs 01 and 02 and the combined umbrella sampling of Ac-Ala-NHMe yield similar result, with maximum deviation for ϕ and ψ of 10°. The free energies of the minima are also consistent, with maximum deviation of the combined run from runs 01 or 02 of 0.3 kcal/mol for the minima and 0.5 kcal/mol for the bridging regions. The ϕ and ψ angles of the minima of runs 01 and 02 and the combined run for Act-Alat-NHMe are also similar, all the angles have a maximum deviation of 10°. The free energies for Act-Alat-NHMe are also consistent, with maximum difference between the combined run and runs 01 or 02 of 0.6 kcal/mol. The larger error associated with Act-Alat-NHMe is consistent with the lower rate of crossovers between the minima.

The high rate of crossover between relative free energy minima on the (ϕ, ψ) map and the good concordance of the results between the two runs is indicative that there was

Table 1
Relative free energy minima and other interesting points from molecular dynamics runs 01 and 02 and the results from the combination of the two runs[a]

	Run 01			Run 02			Combined runs 01 and 02		
	ϕ (°)	ψ (°)	Free energy (kcal/mol)	ϕ (°)	ψ (°)	Free energy (kcal/mol)	ϕ (°)	ψ (°)	Free energy (kcal/mol)
Ac-Ala-NHMe									
β	**−80**	**160**	**0.0**	**−80**	**160**	**0.0**	**−80**	**160**	**0.0**
ε	−150[b]	160[b]	0.6	−150[b]	160[b]	0.3	−150[b]	160[b]	0.4 ± 0.2
α_R	**−70**	**−40**	**0.4**	**−70**	**−40**	**0.8**	**−70**	**−40**	**0.6 ± 0.2**
α_L	**60**	**60**	**1.5**	60	60	2.1	**60**	**60**	**1.8 ± 0.3**
C^7_{axial}	80	−50[b]	2.7	80[b]	−50[b]	3.2	80[b]	−50[b]	3.0 ± 0.3
(−160, −60)	**−160**	**−60**	**1.1**	−160[b]	−60[b]	1.6	−160[b]	−60[b]	1.3 ± 0.3
Bridge 1	0[b]	100[b]	6.2	0[b]	100[b]	6.8	0[b]	100[b]	6.5 ± 0.3
Bridge 2	10[b]	−80[b]	8.4	10[b]	−90[b]	7.8	10[b]	−90[b]	7.9 ± 0.5
Act-Alat-NHMe									
β	**80**	**130**	**0.0**	**80**	**130**	**0.0**	**−80**	**130**	**0.0**
α_R	**−70**	**−30**	**0.3**	**−70**	**−30**	**1.1**	**−70**	**−30**	**0.6 ± 0.5**
(70, −20)	70	−30	3.4	70	−20	3.2	70	−20	3.3 ± 0.1
(70, −110)	70	−110	3.3	70	−110	3.7	70	−110	3.5 ± 0.2
(−160, −70)	−150[b]	−60[b]	2.2	**−160**	**−60**	**1.4**	**−160**	**−70**	**1.6 ± 0.6**
Bridge 1	10[b]	90[b]	7.7	10[b]	90[b]	7.6	10[b]	90[b]	7.6 ± 0.1
Bridge 2	10[b]	−90[b]	7.8	10[b]	−90[b]	8.6	10[b]	−80[b]	8.4 ± 0.6

[a] The uncertainty is defined as the larger of the differences between the combined run and runs 01 or 02. All minima within 2 kcal/mol of the global minimum are shown in boldface.

[b] Not a minimum as defined in Section 3.

sufficient sampling to allow the relative free energies to be calculated with considerable certainty.

3.2. Decomposition of free energy into enthalpy and entropy components

The change of Helmholtz free energy ΔA can be expressed as a function of internal energy U, entropy S and temperature T [32]

$$\Delta A = \Delta U - T\,\Delta S$$

To understand the free energy map in terms of microscopic interactions, the free energy differences were decomposed into their entropic and potential energy components. The entropic and energetic components could be further divided into peptide–peptide (uu), peptide–water (uv) and water–water (vv) components [32]. Yu and Karplus [55] have concluded that the water–water energy contribution, ΔU_{vv} and the entropic contribution, ΔS_{vv}, exactly cancel for each conformation, as a result the relative free energy becomes

$$\Delta A = \Delta U_{uu} + \Delta U_{uv} + -T(\Delta S_{uu} + \Delta S_{uv})$$

The ΔU_{uu} and ΔU_{uv} components for the four conformations β, α_R, α_L and C_7^{axial} were calculated (see Section 2) and the entropic component $-T\,\Delta S$ were calculated by subtracting the energy components from the free energy (Table 2).

The statistical uncertainties were defined as the standard deviation of the conformational distribution around each local minimum. Since the decomposition values are relative to the β-conformation, error propagation was included in the uncertainty. The statistical uncertainties range from 1.7 to 4.9 kcal/mol for the peptide–peptide energy and range from 2.9 to 8.5 kcal/mol for peptide–water interactions. The large uncertainty is a result of calculating small conformational energy differences between two large energies. For example, the average non-bonded energy for the peptide–water interaction of the extended conformation of Ac-Ala-NHMe is −50 kcal/mol with a standard deviation of 4.5 kcal/mol while the energy of the β-conformation is −53 kcal/mol with a standard deviation of 5 kcal/mol. The energy of the extended conformation relative to the β-conformation is small (3 kcal/mol), however, the uncertainty obtained by error propagated is large (6.6 kcal/mol).

Tobias and Brooks [32] calculated statistical uncertainty from the standard deviations of the averages determined using the method of batch averages with a batch size of 100 data sets. The ranges of the statistical uncertainties obtained are similar to our results. Smythe et al. [56] also decomposed the free energy difference between the α-helix and 3_{10}-helix conformation of Ac-Aib$_{10}$-NHMe in explicit water into peptide–peptide and peptide–water components, the uncertainties were also large, ranging from 0.9 to 7 kcal/mol. Due to the large uncertainties, we followed the previous authors [32,56] in treating any observations from the decomposition results not as conclusions, but as indications.

4. Discussion

4.1. Comparing the relative free energy minima for Ac-Ala-NHMe obtained by umbrella sampling with previous calculations

The relative energy and relative free energy for all of the local minima and some interesting conformations are summarized in Table 3. The results show our calculations predict three free-energy minima (β, α_R and α_L) for

Table 2
Decomposition of the terms contributing to the relative free energy of local minima for Ac-Ala-NHMe and Act-Alat-NHMe

	Peptide–peptide				Peptide–water			Total ΔH[a]	Helmholtz free energy, ΔA	Entropy, $-T\,\Delta S$[a]
	Coulombic	van der Waals	Non-bonded	Internal	Coulombic	van der Waals	Non-bonded			
Ac-Ala-NHMe										
β	0 ± 2.4	0.0 ± 2.3	0.0 ± 3.3	0.0 ± 4.8	0.0 ± 8.0	0.0 ± 4.0	0.0 ± 6.8	0.0	0.0	0.0
α_R	0.4 ± 2.9	−0.2 ± 2.2	0.1 ± 3.5	2.4 ± 4.9	−1.7 ± 8.3	−0.2 ± 4.0	−2.0 ± 7.3	0.5	0.6 ± 0.2	0.1
α_L	3.6 ± 2.8	−0.5 ± 2.3	3.1 ± 3.4	2.3 ± 4.8	−5.9 ± 8.4	0.4 ± 4.0	−5.5 ± 7.3	−0.1	1.8 ± 0.3	1.9
ε	−1.6 ± 2.0	0.7 ± 2.3	−0.9 ± 3.0	−0.9 ± 4.7	4.1 ± 7.9	−0.8 ± 4.1	3.3 ± 6.6	1.5	0.4 ± 0.2	−1.1
Ac-Ala-NHMe [32]										
β	0.0[b]				0.0[c]			0.0	0.0	0.0
α_R	11.8[b]				−15.9[c]			−4.1	0.2	4.3
α_L	13.8[b]				−18.4[c]			−4.6	4.1	8.7
C_7^{axial}	2.7[b]				0.8[c]			3.5	3.6	0.1
Act-Alat-NHMe										
β	0.0 ± 3.1	0.0 ± 1.7	0.0 ± 4.1	0.0 ± 3.4	0.0 ± 8.1	0.0 ± 3.1	0.0 ± 7.9	0.0	0.0	0.0
α_L	2.9 ± 3.2	0.6 ± 1.8	3.4 ± 4.2	−0.3 ± 3.3	−4.5 ± 8.5	−0.7 ± 3.1	−5.3 ± 8.3	−2.1	0.6 ± 0.5	2.7
C_7^{axial}	−5.3 ± 3.3	1.1 ± 1.9	−4.2 ± 4.1	7.4 ± 3.5	10.9 ± 7.9	−1.7 ± 2.9	9.3 ± 7.6	12.5	3.3 ± 0.1	−9.2
ε	−3.8 ± 3.1	1.1 ± 1.8	−2.6 ± 3.8	1.1 ± 3.5	8.3 ± 7.1	−1.7 ± 3.1	6.7 ± 7.1	5.1	1.2 ± 0.5	−3.9

[a] Uncertainty was not calculated directly, but it can be obtained from error propagation.
[b] Total peptide–peptide.
[c] Total peptide–water.

Table 3
The ϕ, ψ dihedral angles, energy and free energy of all the minima of Ac-Ala-NHMe and Act-Alat-NHMe[a]

	Diel = 1			Diel = 80			Combined			Anderson and Hermans [34]			Tobias and Brooks [32]		
	ϕ (°)	ψ (°)	Free energy (kcal/mol)	ϕ (°)	ψ (°)	Free energy (kcal/mol)	ϕ (°)	ψ (°)	Free energy (kcal/mol)	ϕ (°)	ψ (°)	Free energy (kcal/mol)	ϕ (°)	ψ (°)	Free energy (kcal/mol)
Ac-Ala-NHMe															
β	−80[b]	160[b]	0.0	**−76**	**150**	**0.0**	**−80**	**160**	**0.0**	**−110**	**120**	**0.0**	**−80**	**120**	**0.0**
ε	**−150**	**160**	**−2.0**	−166[b]	151[b]	0.1	−150[b]	160[b]	0.4 ± 0.2						
α_R	−70[b]	40[b]	1.8	−76[b]	−60[b]	0.8	**−70**	**−40**	**0.6 ± 0.2**	**−120**	**−40**	**1.5**	**−80**	**−60**	**0.2**
α_L	60[b]	60[b]	4.5	59	75	0.4	60	60	1.8 ± 0.3	60	100	2.5	60	60	4.1
C_7^{axial}	**70**	**−60**	**−2.6**	74[b]	−105[b]	2.0	80[b]	−50[b]	3.0 ± 0.3	70	−60	2.7	60	−80	3.6
(−160, −60)	−160[b]	−60[b]	−2.4	**−165**	**−60**	**0.6**	−160[b]	−60[b]	1.3 ± 0.3						
Bridge 1	0[b]	100[b]	7.5	−1[b]	104[b]	5.6	0[b]	100[b]	6.5 ± 0.3						
Bridge 2	10[b]	−90[b]	7.2	14[b]	−90[b]	6.8	10[b]	−90[b]	7.9 ± 0.5						
Act-Alat-NHMe															
β	−81[b]	127[b]	0.0	**−66**	**128**	**0.0**	**−80**	**130**	**0.0**						
α_R	−66[b]	−38[b]	4.6	**−66**	**−37**	**1.3**	**−70**	**−30**	**0.6 ± 0.5**						
ε	**−156**	**127**	**−1.6**	**−156**	**128**	**1.8**	−160[b]	120[b]	1.2 ± 0.6						
α_L	69[b]	80[b]	14.2	69	67	3.4	70[b]	80[b]	4.3 ± 0.2						
C_7^{axial}	**69**	**−39**	**−0.1**	69[b]	−23[b]	4.3	70	−20	3.3 ± 0.1						
(60, −110)	54[b]	−114[b]	4.2	54	−128	2.5	70	−110	3.5 ± 0.2						
(−160, −60)	−156[b]	−54[b]	4.9	−156	−52	3.2	**−160**	**−70**	**1.6 ± 0.6**						
Bridge 1	8[b]	97[b]	13.3	9[b]	98[b]	5.8	10[b]	90[b]	7.6 ± 0.1						
Bridge 2	9[b]	−84[b]	10.8	−6[b]	−82[b]	6.3	10[b]	−80[b]	8.4 ± 0.6						

[a] Some conformations other than minima are also included. The minima which are within 2 kcal/mol of the global minimum are shown in boldface.
[b] Not a minimum as defined in Section 3.

Ac-Ala-NHMe, whereas Tobias and Brooks [32] and Anderson and Hermans [34] predicted four free energy minima (β, α_R, α_L and C_7^{axial}). The extra C_7^{axial} minimum was predicted by Anderson and Hermans [34] and Tobias and Brooks [32] to have a free energy of 2.7 and 3.6 kcal/mol relative to the β-conformation, respectively. The population plot of the ϕ, ψ angles observed experimentally [57] (http://www.ludwig.edu.au/archive/tran) did not show significant population at the C_7^{axial} region, which is more consistent with the results of our calculations. All three relative free energy calculations, Tobias and Brooks [32], Anderson and Hermans [34] and the present work show the β region as the global minimum and the α_R region as the next lowest minimum. In the Tobias and Brooks [32] calculations, the relative free energy for α_R region is 0.2 kcal/mol relative to the β-conformation whereas Anderson and Hermans [34] reports a 1.5 kcal/mol difference. The result of the calculation reported here is 0.6 kcal/mol. The free energy of the α_L conformation relative to the β-conformation is 4.1 kcal/mol according to Tobias and Brooks [32] and 2.5 kcal/mol according to Anderson and Hermans [34]. The result of the calculation reported here (1.8 kcal/mol) is lower than these two studies.

The ϕ and ψ angles of the relative free energy minima calculated here differ by as much as 50° from the ϕ and ψ angles calculated by Anderson and Hermans [34] and Tobias and Brooks [32] (see Table 3). However, the (ϕ, ψ) conformational free energy map (Fig. 3) shows that these region are shallow energetically. Therefore, even with the large deviations in the ϕ and ψ angles of the minima, the energies of the minima are still within approximately 1 kcal/mol of each other.

4.2. Comparing (ϕ, ψ) conformational energy maps with (ϕ, ψ) conformational free energy maps for Ac-Ala-NHMe and Act-Alat-NHMe

The overall shape of the (ϕ, ψ) conformational free energy map for Ac-Ala-NHMe and Act-Alat-NHMe (Fig. 3) is similar to the (ϕ, ψ) conformational energy map calculated using dielectric of 80 [26]. All the ϕ and ψ angles of the minima of the energy maps are all within 16° from the minima found in the free energy maps for Ac-Ala-NHMe (see Table 3). For Act-Alat-NHMe, apart from the fact that the α_L minimum in the energy surface is shifted toward the C_7^{axial} minimum on the free energy surface, the ϕ and ψ angles of the other local minima on the two surfaces are within 20° of each other (Table 3). Considering the large grid being used for the ϕ, ψ maps (15° for the energy maps and 10° for the free energy maps), the ϕ and ψ values of minima for the energy map are practically identical to the ϕ and ψ values of minima for the free energy maps. The similarity between the ϕ and ψ angles of the energy and the free energy maps indicate that the usage of dielectric of 80 to simulate water is a reasonable assumption when attempting to predict the conformations of local free energy minima.

In the relative energy map [26], the (−165, −60) and the α_R conformations were considered as one minimum because the energy barrier between them is less than kT. We refer to this broaden minimum as α_{RB}. In the relative free energy map (Fig. 3), the (−165, −60) conformation was also seen and again was subsumed into α_{RB} because the energy barrier between the (−165, −60) conformation and the α_R conformation was less than kT. The relative energy calculations and the relative free energy calculations predicted opposing relative stability of the (−165, −60) and the α_R conformations. The relative energy calculations with dielectric of 80 predicted that the (−165, −60) conformation is more stable by 0.2 kcal/mol whereas the relative free energy calculations predicted the α_R conformation is more stable by 0.7 kcal/mol, a difference of 0.9 kcal/mol when explicit water and free energy calculation are considered. Since the (−165, −60) conformation is rarely seen experimentally [57] (http://www.ludwig.edu.au/archive/tran), this suggests that the explicit water and free energy calculations are required to model the relative conformation between the (−165, −60) and the α_R conformations more accurately. However, this is not conclusive because the experimental (ϕ, ψ) distribution is not a density distribution of alanine dipeptide, but of alanine in proteins environment obtained from PDB [58,59].

In order from lowest to highest, the relative energy's minima are β (0 kcal/mol), α_L (0.4 kcal/mol) and α_{RB} (0.6 kcal/mol). The relative free energy's minima are β (0 kcal/mol), α_{RB} (0.6 kcal/mol) and α_L (1.8 kcal/mol) (Table 3). The differences between the relative energy and relative free energy are quite small for the β, C_5, α_R and (−160, −60) conformations: 0.0, 0.3, −0.2, and 0.6 kcal/mol, respectively (Table 3). The differences for the two conformations with $\phi > 0$, the α_L and the C_7^{axial} conformations are more significant, being +1.4 and +1.0 kcal/mol, respectively. The transition state, bridges 1 and 2 regions are predicted to have higher barriers (by 0.9 and 1.1 kcal/mol) according to the free energy calculations compared to the energy calculations. Some large differences between the relative free energies and relative energies of the minima and bridging regions of Ac-Ala-NHMe and Act-Alat-NHMe indicate that explicit water and free energy calculations are required to predict the relative stability of conformations.

The decomposition of the terms contributing to the free energy in Table 2 shows that the total peptide–peptide energy component (ΔU_{uu}) of the free energy, followed the basic trend of the (ϕ, ψ) energy map calculated at dielectric of 1. For Ac-Ala-NHMe, the ΔU_{uu} for the β, α_R, α_L and the C_5 conformations are 0.0, 2.5, 5.4 and −1.8 kcal/mol, respectively. Despite the large uncertainty in these values, they are of similar magnitude as the energies calculated using a dielectric constant of 1: 0.0, 1.8, 4.5 and −2.0 kcal/mol, respectively. For Act-Alat-NHMe, the ΔU_{uu} component for the β, α_R, α_L and C_5 conformations are 0, 3.1, 3.2 and −1.6 kcal/mol, respectively. This compares favorably to the results from dielectric of 1 calculations, where the respective

conformational energy are 0, 4.6, 3.5 and −1.6 kcal/mol. The peptide–water energy component (ΔU_{uv}) is related to the solvation energy which have been estimated by a large number of methods [28–33]. The trend for the solvation energies of different dipeptide conformations have been previously explained in terms of the net dipoles of each conformation [60]. The dipoles formed by the two peptide units effectively cancel in the $\phi = -\psi$ region of the (ϕ, ψ) maps. In the $\phi + \psi = \pm 180^\circ$ regions, the dipoles are in phase and, therefore, yield a large net dipole. The C_7^{axial}, $C_7^{equatorial}$ and C_5 regions are in the $\phi = -\psi$ region with minimum net dipole, so the α_R and α_L regions yield more favorable solvation energies.

The peptide–water energy component (ΔU_{uv}) of the free energy calculated here followed the basic trends of solvation energy as explained above and, therefore, can be explained by the net dipole of each conformation. All the ΔU_{uv} in Table 2 are relative to the β-conformation, which exhibit imperfect alignment of the two peptide dipoles of the dipeptide. For Ac-Ala-NHMe, the two peptide dipoles of C_5 conformation cancel out, so there is 3.3 kcal/mol less (relative to the β-conformation) contribution to conformational stability from the peptide–water interaction. The α_L and α_R conformations have aligned peptide unit dipoles, thus the peptide–water interactions are favored by 2.0 and 5.5 kcal/mol, respectively, relative to the β-conformation. The ΔU_{uv} component of the relative free energy of Act-Alat-NHMe also follow similar trend.

The change in entropy, ΔS can be partitioned into two components, peptide–peptide and peptide–water. Brady and Karplus [61] have used MD to estimate the probability density for important internal coordinates (bond, angles, torsional angles or out-of-plane angles) of Ac-Ala-NHMe. Furthermore, they assumed quasi-harmonic approximation to calculate entropy difference between any two conformations. They found that the differences in peptide–peptide entropies between conformations are usually small, even the difference between an internally hydrogen bonded $C_7^{equatorial}$ conformation and non-hydrogen bonded conformation like C_5 or P_{II} is less than 0.5 kcal/mol. Therefore, the change in entropy is mainly due to the change in the peptide–water entropy term. Relative to the β-conformation, the α_R and α_L conformations of Ac-Ala-NHMe and the α_R conformation of Act-Alat-NHMe have increased 'binding' water as seen from the negative peptide–water interaction energy, consequently they are disfavored entropically. For the C_5 conformation of Ac-Ala-NHMe and the C_7^{axial} and C_5 conformations of Act-Alat-NHMe, there is decrease in peptide–water interaction which corresponds to a decreased 'binding' to water and, therefore, the interaction is entropically favored.

4.3. Comparing (ϕ, ψ) conformational free energy maps for Ac-Ala-NHMe and Act-Alat-NHMe

The effects of thio-substitution on the conformation of dipeptides have been examined at the energy level [26]. We concluded that the major effects of thio-substitution are the appearance of four disfavored regions near $\phi = -120$, $\psi = 60$, -60 and 180 and the broadening of the disfavored region near $\phi = 0$ and -120. These disfavored regions are associated with increased overlap between the introduced sulfur atoms and other atoms and, therefore, most likely caused by steric hindrance. The primary differences between the free energy maps of Ac-Ala-NHMe and Act-Alat-NHMe can also be attributed to these disfavored regions.

The notation (x, y, z) is used here to represents the ϕ dihedral angle, ψ dihedral angle and the relative energy in kcal/mol, respectively. In order from lowest to highest relative free energy, the Ac-Ala-NHMe minima are β (−80°, 160°, 0.0 kcal/mol), α_R (−70°, −40°, 0.6 kcal/mol) and α_L (60°, 60°, 1.8 kcal/mol). Act-Alat-NHMe have the following minima: β (−80°, 130°, 0.0 kcal/mol), α_R (−70°, −30°, 0.6 kcal/mol), (−160°, −70°, 1.6 kcal/mol), (70°, −20°, 3.3 kcal/mol) and (70°, −110°, 3.5 kcal/mol) (see Fig. 3 and Table 3).

It may appear that Act-Alat-NHMe is more flexible because it has a higher number of minima. However, upon closer inspection, the latter two minima of Act-Alat-NHMe (70°, −20°, 3.3 kcal/mol) and (70°, −110°, 3.5 kcal/mol), have greater than 3 kcal/mol free energy relative to the β minima and, therefore, they are not expected to be occupied under normal circumstances. Hence, the thio-substitutions restricted the available conformations to the $\phi < 0$ regions. Furthermore, within the $\phi < 0$ region, the conformations available to thio-substituted Act-Alat-NHMe are more restricted than the Ac-Ala-NHMe because of the steeper minima at the β and α_R regions.

The β-conformation of the relative free energy map for Act-Alat-NHMe is less extended than that of Ac-Ala-NHMe (see Fig. 3 and Table 3), i.e. the ϕ angle is the same (−80°) but the ψ angle for Act-Alat-NHMe is smaller, 130° compared to 160° for Ac-Ala-NHMe. This is consistent with the disfavored region near $\psi = 180$. The C_5 region of the (ϕ, ψ) relative free energy maps for both the Ac-Ala-NHMe and Act-Alat-NHMe are subsumed into the β-conformation because the free energy barrier between the two conformations is less than kT. The meta-stable C_5 (−150°, 160°, 0.6 kcal/mol) is shifted to (−160°, 120°, 1.2 kcal/mol) and disfavored by 0.6 kcal/mol (relative to β-conformation) following thio-substitution. The shift of the ψ angle from 160 to 120° is consistent with quantum consideration [25,26] of the C_5 region as well as the addition of the disfavored region near $\psi = -180$ caused by thio-substitution. The shift of the ϕ angle from −150 to −160° is consistent with the disfavored region near $\phi = -120$.

The ϕ angles of the relative free energy minimum at the α_R conformation remained the same with thio-substitution, however, the ψ angle increased from −40 to −30°. This is also consistent with the addition of the disfavored region near $\psi = -60$ upon thio-substitution. The (−160, −60) conformation in the relative free energy surface for Ac-Ala-NHMe

is subsumed into the α_R conformation because the free energy barrier between them is less than kT (see Fig. 3). For Act-Alat-NHMe, the disfavored region near $\phi = -120$ is associated with the increased free energy barrier between the $(-160, -60)$ conformer and the α_R $(-70, -60)$ conformer. Consequently, the two thiopeptide conformers are in distinct free energy minima.

In the Ac-Ala-NHMe free energy map, a minimum is seen in the α_L region (60°, 60°, 1.8 kcal/mol), however, upon thio-substitutions, this minimum no longer exist and new minima appeared at (70°, −20°, 3.3 kcal/mol) and (70°, −110°, 3.5 kcal/mol) (see Fig. 3). Possibly, the disfavored region near $\psi = 60$ upon thio-substitution disfavored the α_L region and consequently, the relatively high-energy regions at (70°, −20°) and (70°, −110°) became minima. This observation is not seen in the conformational energy map.

The free energy of bridges 1 and 2 regions increased by 1.1, and 0.5 kcal/mol, respectively, upon thio-substitutions. This is most likely a consequence of the disfavored region near $\psi = -60$ and near $\phi = 0$. Comparing the free energy calculation and the conformational energy calculation, the free energy calculation predicts increased energy barrier in the bridging regions upon thio-substitution.

5. Conclusions

A single window umbrella sampling technique has been used to determine the (ϕ, ψ) conformational free energy maps for Ac-Ala-NHMe and Act-Alat-NHMe. The technique allowed sampling of the whole free energy surface of dipeptides, including all of the minima, the transition states and other intermediate states. The ϕ and ψ angles for the minima in the relative energy maps calculated with dielectric of 80 are similar to the corresponding ϕ and ψ angles in the relative free energy maps for both Ac-Ala-NHMe and Act-Alat-NHMe. This suggests that the usage of dielectric constant of $\varepsilon = 80$ as approximation of water and the usage of constrained minimization is a reasonable assumption to identify the minima conformations for Ac-Ala-NHMe and Act-Alat-NHMe. However, some large differences between the relative energy and relative free energy of major minima indicate that the consideration of free energy is important in determination of the relative stability of particular minima.

Despite the large uncertainties in the decomposition results, the peptide–peptide energetic components of the free energy are very similar to the energy obtained with dielectric of 1. The peptide–water energetic component of the free energy can be explained qualitatively by the molecular dipole that is formed by the vector addition of the dipoles of the two peptide subunits. Moreover, the peptide–water interaction energy (binding to water), was used qualitatively to explain the entropy contribution. Increased binding to water correlated well with decreased in entropy stabilization and vice versa.

The effects of thio-substitution on conformations of dipeptides were examined by comparing the Ac-Ala-NHMe and Act-Alat-NHMe free energy maps. Thio-substitution appears to restrict the available conformations to the $\phi < 0$ regions. Furthermore, the $\phi < 0$ regions were more restricted because of the deeper β and α_R minima. The changes in the position and relative stability of minima were explained in terms of the destabilization of the regions near $\phi = -120$, 0 and 120, $\psi = 60$, -60, 180, which correspond to the overlaps of the atoms S_{n-1}–$H_{\beta'}$, S_{n-1}–P_n, S_{n-1}–O_β, S_n–C_β, S_n–$H_{\beta'}$ and S_n–P_{n-1}, respectively (P_{n-1} is the peptide bond at the N-terminal and P_n is the peptide bond at the C-terminal).

Acknowledgements

We thank A.E. Mork, for valuable discussion during the design phase of this work.

References

[1] A.F. Spatola, Chemistry and Biochemistry of Amino Acids, Peptides and Proteins, Marcel Dekker, New York, 1983, pp. 267–357.
[2] A.G. Michel, C. Ameziane-Hassani, G. Boulay, Structural study of the thioamide bond: synthesis and conformation of derivatives of thioalanine and thioglycine, Can. J. Chem. 67 (1989) 1312–1318.
[3] W.L. Mock, J.T. Chen, J.W. Tsang, Hydrolysis of thiopeptide by cadmium carboxypeptidase A, Biochem. Biophy. Res. Commun. 102 (1981) 389–396.
[4] L.D. Rutledge, J.H. Perlman, M.C. Gershengorn, G.R. Marshall, K.D. Moeller, Conformationally restricted TRH analogs: a probe for the pyroglutamate region, J. Med. Chem. 39 (8) (1996) 1571–1574.
[5] P. Juvvadi, D.J. Dooley, C.C. Humblet, G.H. Lu, E.A. Lunney, R.L. Panek, R. Skeean, G.R. Marshall, Bradykinin and angiotensin II analogs containing a conformationally constrained proline analog, Int. J. Peptide Protein Res. 40 (1992) 163–170.
[6] J. Turk, G.R. Marshall, α-Methyl substrates of carboxypeptidase A. A steric probe of the active site, Biochemistry 14 (12) (1975) 2631–2635.
[7] B.V.V. Prasad, P. Balaram, The stereochemistry of peptides containing α-aminoisobutyric acid, CRC Crit. Rev. Biochem. 16 (4) (1983) 307–348.
[8] I.L. Karle, J.L. Flippen-Anderson, M. Sukumar, K. Uma, P. Balaram, Modular design of synthetic protein mimics. Crystal structure of two seven-residue helical peptide segments linked by ε-aminocaproic acid, J. Am. Chem. Soc. 113 (1991) 3952–3956.
[9] W.F. Degrado, D.P. Raleigh, T. Handel, De novo protein design. What are we learning? Curr. Opin. Struct. Biol. 1 (1991) 984–993.
[10] A.W. Burgess, S.J. Leach, An obligatory α-helical amino acid residue, Biopolymers 12 (1973) 2599–2605.
[11] G.R. Marshall, H.A. Bosshard, Angiotensin II. Biologically active conformation, Circ. Res. 30/31 (Supp. II) (1972) 143.
[12] K. Ramnarayan, M.F. Chan, V.N. Balaji, S.J.R. Profeta, S.N. Rao, Conformational studies on model dipeptides of Gly, L-Ala and their C alpha-substituted analogs, Int. J. Peptide Protein Res. 45 (1995) 366–376.
[13] D.H. Apella, L.A. Christianson, I.L. Karle, D.R. Powell, S.H. Gellman, β-Peptide foldamers: robust helix formation in a new family of β-amino acid oligomers, J. Am. Chem. Soc. 118 (1996) 13071–13072.

[14] D. Seebach, M. Overhand, F.N.M. Kuhnle, B. Martinoni, L. Oberer, U. Hommel, H. Wdimer, Beta-peptides — synthesis by Arndt–Eistert homologation with concomitant peptide coupling — structure determination by NMR and CD spectroscopy and by X-ray crystallography — helical secondary structure of a beta-hexapeptide in solution and its stability towards pepsin (review), Helv. Chim. Acta 79 (1996) 913–941.

[15] R.J. Simon, R.S. Kania, R.N. Zuchermann, V.D. Huebner, D.A. Jewell, S. Banville, S. Ng, L. Wang, S. Rosenberg, C.K. Marlowe, Peptides: a molecular approach to drug discovery, Proc. Natl. Acad. Sci. U.S.A. 89 (1992) 9367–9371.

[16] A. Aubury, J. Protas, G. Boussard, M. Marraud, J. Neel, Experimental conformational study of two peptides containing α-aminoisobutyric acid. Crystal structure of *N*-acetyl-α-aminoisobutyric acid methylamide, Biopolymers 17 (1978) 1693–1711.

[17] Y. Paterson, S.M. Rumsey, E. Benedetti, G. Nemethy, H.A. Scheraga, Sensitivity of polypeptide conformation to geometry. Theoretical conformational analysis of oligomers of α-aminoisobutyric acid, J. Am. Chem. Soc. 103 (1981) 2947–2955.

[18] D.F. Veber, R.M. Freidinger, D.S. Perlow, W.J. Paleveda, F.W. Holly, R.G. Strachan, R.F. Nutt, B.H. Arison, C. Homnick, W.C. Randall, M.S. Glitzer, R. Saperstein, R. Hirschmann, A potent cyclic hexapeptide analogue of somatostatin, Nature 292 (1981) 55–58.

[19] D.F. Veber, F.W. Holly, R.F. Nutt, S.J. Bergstrand, S.F. Brady, R. Hirschmann, Highly active cyclic and bicyclic somatostatin analogues of reduced ring size, Nature 280 (1979) 512–514.

[20] H.A.S. Hansen, K. Clausen, T.F.M. La Cour, Structure of the dithiopeptide (*Z*)-Glyt-Glyt-Gly-Obzl, Acta Crystallogr. C 43 (1987) 522–524.

[21] T.F.M. La Cour, Stereochemistry of peptides containing a thioacyl group, Int. J. Peptide Protein Res. 30 (1987) 564–571.

[22] T.F.M. La Cour, H.A.S. Hansen, K. Clausen, S.O. Lawesson, The geometry of the thiopeptide unit, Int. J. Peptide Protein Res. 22 (1983) 509–512.

[23] H.A.S. Hansen, K. Clausen, T.F.M. La Cour, Structure of thiopeptide (*Z*)-Glyt-Gly-Obzl, Acta Crystallogr. C 43 (1987) 519–522.

[24] V.N. Balaji, S.J.R. Profeta, S.W. Dietrich, Mean geometry of the thiopeptide unit and conformational features of dithiopeptides and polythiopeptides, Biochem. Biophy. Res. Commun. 145 (1987) 834–841.

[25] T.T. Tran, H.R. Treutlein, A.W. Burgess, Conformational analysis of thiopeptides: derivation of sp^2 sulfur parameters for the CFF91 force field, J. Comput. Chem. 22 (2001) 1010–1025.

[26] T.T. Tran, H.R. Treutlein, A.W. Burgess, Conformational analysis of thiopeptides: (ϕ, ψ) maps of thio-substituted dipeptides, J. Comput. Chem. 22 (2001) 1026–1037.

[27] T.T. Tran, H.R. Treutlein, A.W. Burgess, J. Perich, Synthesis, X-ray crystallographic structures of thio-substituted *N*-acetyl-*N*′-methylamide alanine and testing of sp^2 sulfur parameters of the CFF91 force field, J. Pep. Res. 58 (2001) 67–78.

[28] A. Jean-Charles, A. Nicholls, K. Sharp, B. Honig, A. Tempczyk, T.F. Henderson, W.C. Still, Electrostatic contributions to solvation energies: comparison of free energy perturbation and continuum calculations, J. Am. Chem. Soc. 113 (1991) 1454–1455.

[29] W.C. Still, A. Tempczyk, R.C. Hawley, T. Hendrickson, Semi-analytical treatment of solvation for molecular mechanics and dynamics, J. Am. Chem. Soc. 112 (1990) 6127–6129.

[30] B.M. Pettitt, M. Karplus, The potential of mean force surface for the alanine dipeptide in aqueous solution: a theoretical approach, Chem. Phys. Letters 121 (1985) 194–201.

[31] B.M. Pettitt, M. Karplus, Conformational free energy of hydration for alanine dipeptide: thermodynamic analysis, J. Phys. Chem. 92 (1988) 3994–3997.

[32] D.J. Tobias, C.L. Brooks III, Conformational equilibrium in the alanine dipeptide in the gas phase and aqueous solution: a comparison of theoretical results, J. Phys. Chem. 96 (1992) 3864–3870.

[33] M. Mezei, P.K. Mehrotra, D.L. Beveridge, Monte Carlo determination of the free energy and internal energy of hydration of the alanine dipeptide at 25°C, J. Am. Chem. Soc. 107 (1985) 2239–2245.

[34] A.G. Anderson, J. Hermans, Microfolding: conformational probability map for the alanine dipeptide in water from molecular dynamics simulations, Prot.: Struct. Funct. Genet. 3 (1988) 262–265.

[35] A.R. Leach, Molecular Modeling, Principles and Applications, Addison-Wesley, Longman, UK, Singapore, 1996.

[36] R.W. Zwanzig, High-temperature equation of state by a perturbation method. I. Nonpolar gases, J. Chem. Phys. 22 (1954) 1420–1426.

[37] G.M. Torrie, J.P. Valleau, Nonphysical sampling distributions in Monte Carlo free-energy estimation: umbrella sampling, J. Comput. Phys. 23 (1977) 187–199.

[38] F. Fraternali, W.F. van Gunsteren, Conformational transitions of a dipeptide in water: effects of imposed pathways using umbrella sampling techniques, Biopolymers 34 (1994) 347–355.

[39] D.J. Tobias, S.F. Sneddon, C.L. Brooks III, Reverse turns in blocked dipeptides are intrinsically unstable in water, J. Mol. Biol. 216 (1990) 783–796.

[40] P.W. Atkins, Physical Chemistry, Oxford University Press, Oxford, Melbourne, Tokyo, 1990.

[41] W.L. Jorgensen, J. Chandrasekhar, J.D. Madura, Comparison of simple potential functions for simulating liquid water, J. Chem. Phys. 79 (1983) 926–935.

[42] F.H. Stillinger, A. Rahman, Improved simulation of liquid water by molecular dynamics, J. Chem. Phys. 60 (1974) 1545–1557.

[43] J.D. Bernal, R.H. Fowler, J. Chem. Phys. 1 (1933) 515.

[44] H.C. Berendsen, J.P.M. Postma, W.F. van Gunsteren, J. Hermans, Intermolecular Forces, Pullman, Dordrecht, Reidel, 1981, pp. 331–342.

[45] M. Hassan, C.S. Ewig, Determining the accuracy and reliability of molecular simulations of nucleic acid systems using the CFF91 force field, Abstr. Pap. Am. Chem. Soc. 213 (1997) 266.

[46] J.R. Maple, M.J. Hwang, T.P. Stockfisch, U. Dinur, M. Waldman, C.S. Ewig, A.T. Hagler, Derivation of class II force fields. I. Methodology and quantum force field for the alkyl functional group and alkane molecules, J. Comput. Chem. 15 (2) (1994) 162–182.

[47] M.J. Hwang, T.P. Stockfisch, A.T. Hagler, Derivation of class II force fields. 2. Derivation and characterization of class II force field, CFF93, for the alkyl functional group and alkane molecules, J. Am. Chem. Soc. 116 (1994) 2515–2525.

[48] J.R. Maple, M.J. Hwang, T.P. Stockfisch, A.T. Hagler, Derivation of class II force fields. 3. Characterization of a quantum force field for alkanes, Isr. J. Chem. 34 (2) (1994) 195–231.

[49] Z.W. Peng, C.S. Ewig, M.J. Hwang, M. Waldman, A.T. Hagler, Derivation of class II force fields. 4. van der Waals parameters of alkali metal cations and halide anions, J. Phys. Chem. A 101 (1997) 7243–7252.

[50] J.R. Maple, M.J. Hwang, K.J. Jalkanen, T.P. Stockfisch, A.T. Hagler, Derivation of class II force fields. 5. Quantum force field for amides, peptides, and related compounds, J. Comput. Chem. 19 (1998) 430–458.

[51] C.S. Ewig, T.S. Thacher, A.T. Hagler, Derivation of class II force fields. 7. Non-bonded force field parameters for organic compounds, J. Phys. Chem. B 103 (1999) 6998–7014.

[52] C.S. Ewig, C. Liang, T.R. Stouch, A.T. Hagler, Development of a class-II (CFF) force field for modeling biomembrane lipids, Abstr. Pap. Am. Chem. Soc. 207 (1994) 109.

[53] S.H. Northrup, M.R. Pear, C.-Y. Lee, J.A. McCammon, M. Karplus, Dynamical theory of activated processes in globular proteins, Proc. Natl. Acad. Sci. U.S.A. 79 (1982) 4035–4039.

[54] CDiscover 2.9.7/95.0/3.00, Force field simulations, User Guide, Part I. Molecular Simulation, 9685 Scranton Road, San Diego, CA, 1995.

[55] H.-A. Yu, M. Karplus, A thermodynamic analysis of solvation, J. Chem. Phys. 89 (1988) 2366–2379.

[56] M.L. Smythe, S.E. Huston, G.R. Marshall, The molten helix: effects of solvation on the α- to 3_{10}-helical transition, J. Am. Chem. Soc. 117 (1995) 5445–5452.
[57] R.H. Flegg, Molecular Modeling Studies, Ph.D. Thesis, 1993.
[58] F.C. Berstein, T.F. Koetzle, G.J.B. Williams, F. Edgar, J. Meyer, M.D. Brice, O. Kennard, T. Shimanouchi, M. Tasumi, The protein data bank: a computer-based archival file for macromolecular structures, J. Mol. Biol. 112 (1977) 535–542.
[59] J.L. Sussman, E.E. Abola, D. Lin, J. Jiang, N.O. Manning, J. Prilusky, The protein data bank, Genetica 106 (1999) 149–158.
[60] C.L. Brooks III, D.A. Case, Simulations of peptide conformational dynamics and thermodynamics, Chem. Rev. 93 (1993) 2487–2502.
[61] J. Brady, M. Karplus, Configuration entropy of the alanine dipeptide in vacuum and in solution: a molecular dynamics study, J. Am. Chem. Soc. 107 (1985) 6103–6105.